SF2A 2006
D. Barret, F. Casoli, T. Contini, G. Lagache, A. Lecavelier, and L. Pagani (eds)

THE SPATIAL DISTRIBUTION OF MOLECULAR SPECIES OBSERVED IN COMET HALE BOPP WITH THE PLATEAU DE BURE INTERFEROMETER

J. Boissier[1], D. Bockelée-Morvan[1], J.-F. Crifo[2] and A. V. Rodionov[3]

Abstract. In March 1997, with the IRAM Plateau de Bure Interferometer, unique data were obtained in comet C/1995 O1 (Hale-Bopp) on several species with angular resolution of 1 to 3". We have developed a model which simulates interferometric observations of spectral lines. This model takes into account the variation of the excitation conditions in the coma and optical depth effects, found to be significant in comet Hale-Bopp. It can accommodate any 3-D molecular spatial distribution and its velocity field as input parameters. We present here the analysis of the observed CO coma structure using physical models of comet Hale-Bopp atmosphere and that of CS and SO radial distribution assuming an isotropic outflow. The traditional (no gas dynamics) analysis of CO observations suggested the presence of a nearly equatorial CO jet spiraling with nucleus rotation and comprising about 40 percent the total CO production (Henry et al. 2002). Rodionov and Crifo (2006) developed a time-dependent 3-D model of comet Hale-Bopp gas coma. They investigated first the case of a homogeneous outgassing of CO and H_2O from a non-spherical rotating nucleus. A second computation considers the same nucleus and H_2O outgassing but assumes the presence of an area with increased CO production on the nucleus surface. We show that the structures created in the first case cannot explain the observations while those detected in the second case are comparable to observed ones. The study of the radial distribution of molecular species can provide constraints on their photodissociation rate, and, for radicals, on that of their parents. These rates are not well known for several species and we present results obtained for CS, SO and SO_2.

1 Introduction

The structure and composition of cometary nuclei may provide constraints on the initial conditions of Solar System evolution. However their study is made difficult when they pass close to the Earth because evaporating gas and dust create a blinding atmosphere. Millimeter radioastronomy is sensitive to the emission of rotational lines of parent products, close to the nucleus, with a good spectral resolution. Interferometric observations offer spatial resolution but require a very high comet activity to be carried out. In 1997, comet C/1995 (Hale-Bopp) was a good target and was observed at the IRAM Plateau de Bure Interferometer (PdBI). As presented in this paper, these data provide informations on the structure of the inner coma and on the radial extension of CS and SO.

2 Observations

Comet C/1995 O1 (Hale-Bopp) was observed in 1997 from March 6 to 22 at the IRAM PdBI, situated in the french Alps, during its approach to the Earth (the perigee was reached on March 22). At this time, the instrument counted five 15-m antennas set in C1 compact configuration so that baseline lengths projected on the plane of the sky were comprised between 22 m and 147 m. The geocentric distance of the comet was about $\Delta \sim 1.35$ AU and the heliocentric $r_h \sim 1$ AU. The observing campaign included interferometric mapping and single dish (autocorrelation) measurements in spectroscopic mode for several molecular species (CO, HCN, HNC, CS, H_2S, SO_2, SO) as well as observations of the dust continuum emission (Altenhoff et al. 1999). The Table 1 summarizes the characteristics of the observations studied in the present work.

[1] Observatoire de Paris, 5 pl. Jules Janssen 92195 Meudon
[2] Service d'Aéronomie, Réduit de Verrières - BP 3 Route des Gatines 91371 Verrières le Buisson Cédex France
[3] Central Research Institute of Machine Building, Pionyerskaya St., 4, Korolev, Moscow region, 141070, Russia

Table 1. Log of the observations and main characteristics

Line	Freq. GHz	Date in March	Mode	Ang. Resol. arcsec (")	Spec. Resol. km.s^{-1}	Line area[a] Jy.km.s^{-1}	Δv[b] km.s^{-1}
CO	230.538	11	cross	2 × 1.38	0.13	4.86 ± 0.17	
J(2-1)			auto	20.9		82.8 ± 0.6	-0.083 ± 0.007
CO	115.271	11	cross	3.57 × 2.6	0.13	1.01 ± 0.07	
J(1-0)			auto	41.8		10.8 ± 0.4	-0.09 ± 0.05
CS	244.936	12	cross	1.92 × 1.28	0.12	5.4 ± 0.7	
J(5-4)			auto	19.7		213 ± 0.6	-0.098 ± 0.003
CS	97.981	12	cross	4.39 × 2.82	0.31	1.45 ± 0.05	
J(2-1)			auto	49		15.2 ± 0.2	-0.08 ± 0.01
SO	219.949	13	cross	1.93 × 1.5	0.14	0.44 ± 0.04	
$N_J(5_6\text{-}4_5)$			auto	21.9		16.9 ± 0.9	-0.15 ± 0.02

[a] Integrated intensity in the main beam for single dish spectra (autocorrelation mode), and in the central pixel of the interferometric maps (cross-correlation mode). The given uncertainty is the error due to the measurement. The absolute calibration adds a 15% uncertainty.

[b] Line velocity shift defined as $\Delta v = \frac{\sum_i T_i v_i}{\sum_i T_i}$ where i represents the channels numbers where the line is present.

3 The CO coma

3.1 Observations

Both interferometric and single dish observations of the line J(2-1) at 230 GHz of CO led to the conclusion that a CO spiral structure was rotating with the nucleus (Henry et al. 2002). On the autocorrelation spectra the mean velocity offset evolves with time, following a sine with the rotation period of the nucleus (11.35 h, Jorda et al. 2000, see Figure 1). The interferometric overall map (8 h observations) is asymmetric, suggesting that the CO outflow is not isotropic. Furthermore, on successive individual maps (data subsets of 1 hour), the position of the brightness maximum moves along the direction perpendicular to the spin axis (Figure 1).

Through phenomenological modeling (no gas dynamics, spherical nucleus), Henry et al. (2002) showed that all these features were consistent with the presence on the nucleus of a low latitude jet comprising $\sim$ 40% the total CO production.

3.2 Coma model

Rodionov and Crifo (2006) suggested that an elongated nucleus could create strong structures in the gas coma during its rotation without any inhomogeneity in gas production on the surface. They developed a 3-D, time dependent, gas dynamics model of a coma created by a non spherical rotating nucleus. The nucleus shape is that of 1/P Halley adapted to Hale-Bopp size and H_2O is assumed to sublimate according to solar illumination while CO diffuses uniformly from below the surface (Solution 1).

In a second step, they included in the model an area with higher CO production on the nucleus surface (Solution 2). The aim was to check whether the "jet" described by Henry et al (2002) could survive gas dynamics effects and still reproduce observations.

3.3 Simulating observations

We developed a model able to simulate radio observations in interferometric and single dish modes from any coma model. In a first step it computes the brightness distribution on the plane of the sky according to the excitation model described in Biver et al. (1999a) and taking into account opacity effects. The synthetic spectra are obtained convolving the brightness distribution with a Gaussian beam. The simulation of interferometric observations is carried out using GILDAS softwares provided by IRAM. Real conditions of observations (interferometer configuration) are used. Simulated data are then processed in the same way as the observations.

3.4 Results

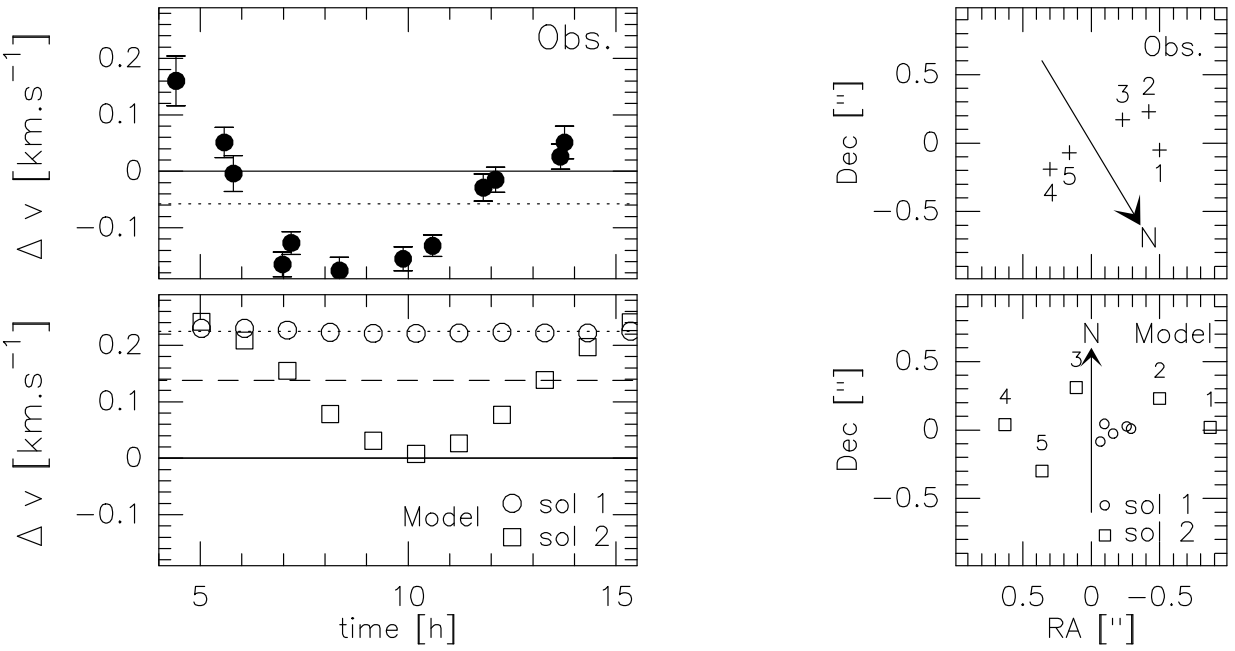

Fig. 1. *Left :* Time evolution of the velocity shift of single dish spectra. *Right :* Position of the brightness maximum on five successive maps observed in interferometric mode. Integration time is one hour centered on 5h (label 1), 6h30 (2), 7h50 (3), 9h20 (4), and 11h15 (5). The observations (respectively the model results) are presented in the top (resp. bottom) panels.

On the single dish spectra, the variation of the velocity offset with Solution 1 ($\sim 0.01\,\mathrm{km\ s^{-1}}$) is about 40 times fainter than observed ($\sim 0.4\,\mathrm{km\ s^{-1}}$). The position of the brightness maximum is almost the same on all the individual maps. With Solution 2, the velocity offset on single dish spectra undergoes variations of $\sim 0.25\,\mathrm{km\ s^{-1}}$. As observed, the position of the brightness maximum is offseted ($\sim 1''$) with respect to the mean position, on the direction perpendicular to the spin axis.

As a conclusion, nucleus shape effects on the coma structure are too faint to be detectable in the observations. Assuming the presence of an area with higher CO production on the nucleus, simulations show that it is possible to reproduce the main features observed in Hale-Bopp with the PdBI in 1997. However the model does not reproduce correctly all the observed features (e. g. line profile, mean velocity offset) and new computations are in progress in order to improve the results.

4 Gas radial extension

4.1 Photodissociation rates

Once released in the coma, parent products undergo photodissociation. The efficiency of this process is given by the photodissociation rate at 1 AU from the Sun (β, [km s^{-1}]), a parameter that is required to derive molecular abundances in comae. The usual way to determine a photodissociation rate is to join lab measurements and theoretical computations. However this method is not accurate enough for some molecular species as SO and CS, for which different values are published in the literature. PdBI observations of Hale-Bopp provide new constraints on their photodissociation rates.

As presented in Table 1, the single dish flux F_{SD} is measured in a beam much larger than the interferometric map center flux F_{Int}. As a result, the ratio $R = \frac{F_{SD}}{F_{Int}}$ probes the radial extension of the molecules in the coma.

In order to constrain β_{CS} and β_{SO}, we tested several values in the model, assuming that the coma is isotropic (Haser density), for comparison with the observations.

4.2 CS

CS is created by the photodissociation of CS_2 in the first 500 kilometers of the coma. Jackson et al. (1982) deduced $\beta_{CS} = 1 \times 10^{-5}\,s^{-1}$ from IUE observations in the UV. Snyder et al. (2001) suggested that it should be ten times higher (1×10^{-4} s^{-1}) according to their analysis of interferometric observations with the Berkeley Illinois Maryland Association (BIMA) array. Single dish observations of comets very close to the Sun (Biver et al. 2004) show that this latter value is too high and suggested $\beta_{CS} = 2 \times 10^{-5}\,s^{-1}$.

In our data, CS is observed through two transitions, J(5-4) at 244 GHz and J(2-1) at 98 GHz, and the observed ratios are $R_{54} = 39 \pm 10$ and $R_{21} = 10.5 \pm 1.8$ respectively. We simulated observations to compute R_{54} and R_{21} for all the published values of β_{CS}. The comparison with the observations shows that the value proposed by Snyder et al. (2001) leads to fluxes ratios ($R_{54} \sim 20$ and $R_{21} \sim 5$) inconsistent with the observed ones. Assuming a variable temperature in the coma (increasing from 20 K at 100 km to 120 K at 10000 km and constant beyond 100000 km) $\beta_{CS} = 1 \times 10^{-5}$ s^{-1} and $\beta_{CS} = 2 \times 10^{-5}$ s^{-1} produce R_{54} and R_{21} values in agreement with observations.

4.3 SO and SO_2

SO is the photodissociation product of SO_2. Different values are found in the literature for both β_{SO} (1.5, 4.9 and $6.2 \times 10^{-4}\,s^{-1}$) and β_{SO_2} (1.4 and $2.1 \times 10^{-4}\,s^{-1}$), as detailed in Bockelée-Morvan et al. (2000). We made model computations with many (β_{SO}, β_{SO_2}) couples to study R as a function of β_{SO} and β_{SO_2} (Figure 2). We cannot deduce any constraint on β_{SO_2} but the only value of β_{SO} producing the observed R is 1.5×10^{-4} s^{-1}.

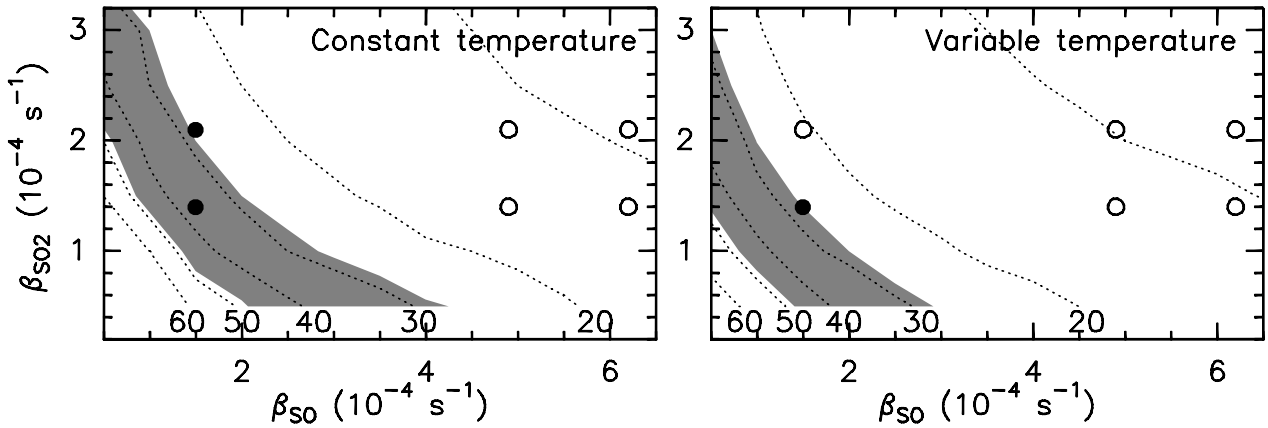

Fig. 2. Single dish to interferometric flux ratio R as a function of β_{SO} and β_{SO_2}. R is represented by the contours which values are indicated in the bottom of the figure. The area where R is in agreement with observations is filled in grey. The circles represent the (β_{SO}, β_{SO_2}) couples found in the literature. $\beta_{SO} = 1.5 \times 10^{-4}$ s^{-1} is the only value that reproduces the observed R, whatever β_{SO_2} and the assumed gas temperature.

References

Biver, N., et al. 1999a, ApJ, 118, 1850
Biver, N., et al. 2003, BAAS, 35, 958
Bockelée-Morvan, D., et al. 2000, A&A, 353, 1101-1114
Henry, F., et al. 2002, EM&P, 90, 57
Jackson, W.M., et al. 1982, A&A, 107, 385
Jorda, L., & Gutiérrez, P. 2000, EM&P, 99, 135
Rodionov, A.V., & Crifo, J.-F. 2006, Adv. Space. Res, in press
Snyder, L.E., et al. 2001, ApJ, 121, 1147